Research Article | Vol. 15, No. 10 / 1 Oct 2025 / Optical Materials Express 2633
Optical Materials EXPRESS

Flatness-insensitive pulsed electric current bonding of sapphire/Nd:YAG ceramics

HIROAKI FURUSE,[1,*] HIROYUKI TANAKA,[2] YUKI KAGAMI,[2] HIYORI UEHARA,[3] AND RYO YASUHARA[3]

[1] *National Institute for Materials Science, 1-2-1 Sengen, Tsukuba, Ibaraki, Japan*
[2] *Kitami Institute of Technology, 165 Koen-cho, Kitami, Hokkaido, Japan*
[3] *National Institute for Fusion Science, 322-6 Oroshi-cho, Toki, Gifu, Japan*
[*] *FURUSE.Hiroaki@nims.go.jp*

Abstract: Initial surface-flatness-insensitive bonding of sapphire and YAG ceramics for high-average-power laser materials was achieved via pulsed electric current bonding (PECB), a type of thermal diffusion bonding. Nd:YAG ceramics with surface flatness of $\lambda/10$, $\lambda/5$, and λ ($\lambda = 632.8$ nm) were bonded to sapphire (flatness $< \lambda/10$). All samples exhibited excellent optical performance irrespective of initial flatness. In-line transmittance approached theoretical limits, transmitted wavefront distortion was below 0.264λ, and polarization exceeded 35 dB. Minor unbonded regions appeared near edges for λ-flat samples, but overall performance remained unaffected. TEM analysis revealed interfacial microstructures, providing deeper insights. These findings demonstrate that PECB enables high-quality bonding with minimal dependence on initial flatness, making it advantageous for manufacturing large-aperture, high-average-power, and high-pulse-energy laser materials.

1. Introduction

The development of high-average-power lasers requires effective management of thermal effects such as thermal lensing, thermal birefringence, and thermal stress fracture, as these issues significantly degrade laser performance. These effects primarily arise from heat accumulation in the laser gain medium and the resulting temperature gradients caused by cooling. Therefore, it is essential to consider both material geometry and cooling techniques in order to effectively mitigate these effects.

One effective approach for thermal management involves bonding the laser medium to highly thermally conductive optical materials, such as diamond [1] or sapphire [2–8], which serve as heatsinks. These composite structures effectively dissipate heat along the optical path and suppress radial temperature gradients.

Surface-activated bonding (SAB) is among the most effective methods for bonding dissimilar optical materials, such as YAG and heatsinks. SAB can be performed at room temperature, making it insensitive to thermal expansion mismatches between different materials and therefore highly suitable for bonding materials with significantly different coefficients of thermal expansion. Prior studies have reported that the damage threshold at the sapphire/YAG interface bonded by SAB is as high as that of the bulk [9], and that the thermal resistance at the interface is negligibly small [10]. Consequently, nanosecond pulses with joule-class pulse energies have been achieved [11]. However, SAB requires stringent conditions, including high-quality initial surfaces (surface flatness less than $\lambda/10$) and ultrahigh vacuum ($\sim 10^{-5}$ Pa) [1,6]. These stringent requirements could limit the scalability of laser media, particularly for larger apertures exceeding 10 cm, which are essential for 100 J-class high-pulse-energy lasers to prevent damage issues [12–14].

Alternative bonding methods for dissimilar optical materials have also been reported, including glass bonding [15,16] and thermal diffusion bonding [3,5]. In glass bonding, significant efforts have been made to minimize degradation of mechanical and optical properties and reducing

#575741 https://doi.org/10.1364/OME.575741
Journal © 2025 Received 9 Aug 2025; revised 24 Sep 2025; accepted 24 Sep 2025; published 1 Oct 2025

Optical Materials EXPRESS

refractive index mismatch at the interface [17–19]. However, improvements in laser performance using this method have remained limited.

With respect to thermal diffusion bonding, to the best of our knowledge, the first successful bonding of Nd:YAG and sapphire, which have different crystal structures, was achieved using pulsed electric current bonding (PECB), also referred to as spark plasma sintering [3]. The resulting enhancement in laser performance has been attributed to the conductive cooling effect of sapphire. Although thermal diffusion bonding of dissimilar materials is generally challenging, the relatively small mismatch in thermal expansion coefficients between sapphire and YAG, combined with the low-temperature (1100°C) and short-time (1 hour) bonding process enabled by uniaxial pressure (64 MPa) in the PECB method, are considered key factors for successful bonding. Compared with SAB, PECB can be performed under moderate vacuum conditions (several Pa) and enables the simultaneous bonding of multiple layers in a single process, making it a simpler and more practical approach. Therefore, PECB is a promising technique for fabricating sapphire/YAG composites.

To extend the applicability of PECB to high-average-power laser materials, a detailed understanding of the required bonding conditions is necessary. In particular, the influence of the initial surface flatness on achieving sufficient optical performance in these composites has not been comprehensively investigated. Clarifying these requirements is crucial for fabricating large-diameter composite laser media for high-pulse-energy lasers. Furthermore, although the previous study has primarily focused on optical transmittance, other critical characteristics have not been systematically examined [3]. Specifically, evaluating transmitted wavefront distortion and stress-induced depolarization is vital for laser applications. Additionally, high-resolution electron microscopy analysis of the bonded interface is essential for optimizing the bonding process.

In this study, we fabricated sapphire/Nd:YAG composite materials with varying initial surface flatness using PECB to investigate the conditions required for successful bonding. The optical characteristics, including transmitted spectra, transmitted wavefront, stress-induced depolarization, and laser performance, were systematically compared. Moreover, the bonded interface microstructure was examined using transmission electron microscopy (TEM) for both sapphire/Nd:YAG ceramic and single-crystal composites to clarify the differences between them.

2. Experimental method

2.1. Pulsed electric current bonding (PECB) of sapphire/ Nd:YAG ceramic composite

The starting materials were commercially available *a*-cut sapphire (Orbe Pioneer Co. Ltd., Japan) and Nd:YAG ceramics (Konoshima Chemical Co. Ltd., Japan), each with dimensions of 10 mm in diameter and 2 mm in thickness. Figure 1 shows a schematic of the sapphire/Nd:YAG composite material.

The bonded surfaces of the Nd:YAG ceramics were polished to approximately λ/10 (two pieces), λ/5 (three pieces), and λ (two pieces), whereas the sapphire surfaces were polished to less than λ/10 (seven pieces), where λ = 632.8 nm. Surface flatness was evaluated based on peak-to-valley (PV) values measured using a laser interferometer (Verifire, ZYGO, USA) and provided by the polishing company. Detailed information on the initial surface flatness of all samples is summarized in Table 1.

After assembling each pair of surfaces, the samples were bonded using a PECB system (Labox-315, Sinter Land Co. Ltd., Japan). The bonding temperature and applied pressure were 1100°C and 64 MPa, respectively, as described in our previous study [3]. After bonding, all surfaces of the composites were polished again for subsequent characterization.

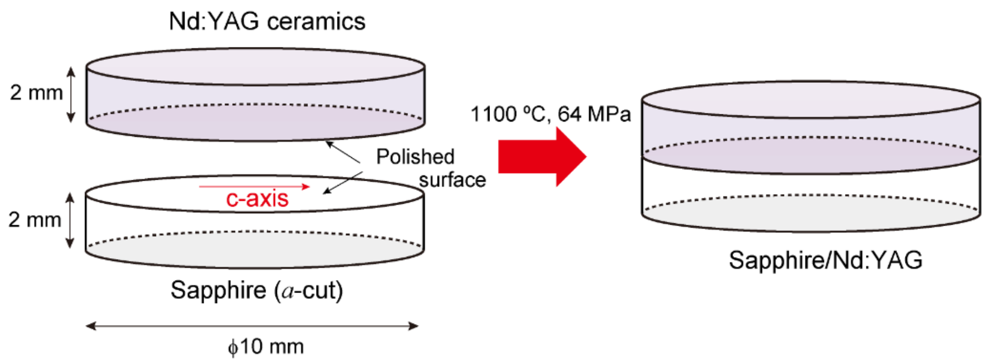

Fig. 1. Schematic of sapphire and Nd:YAG ceramic composite material.

Table 1. Initial surface flatness at the polished surfaces for the composite sample. $\lambda = 632.8$ nm.

	Peak-to-valley values of initial surface flatness (λ)	
Sample	Nd:YAG ceramics	sapphire
Composite-1	0.096 (~ λ/10)	0.033 (< λ/10)
Composite-2	0.096 (~ λ/10)	0.041 (< λ/10)
Composite-3	0.194 (~ λ/5)	0.063 (< λ/10)
Composite-4	0.196 (~ λ/5)	0.071 (< λ/10)
Composite-5	0.198(~ λ/5)	0.041 (< λ/10)
Composite-6	0.973(~ λ)	0.096 (< λ/10)
Composite-7	0.977 (~ λ)	0.036 (< λ/10)

2.2. *Characterization of optical properties*

The transmitted wavefronts (PV values) of all polished sapphire/Nd:YAG composites were also measured by the polishing company using the laser interferometer. Transmission spectra were measured using a UV/VIS/NIR spectrometer (UV-3600 Plus, Shimadzu Co. Ltd., Japan).

The experimental setup for measuring the degree of polarization is shown in Fig. 2. A 632.8 nm linearly polarized He-Ne laser was used as the probe beam. The laser beam was expanded and collimated using two lenses, and the sample was irradiated at normal incidence. The polarizer was adjusted so that the laser polarization aligned with the sapphire *c*-axis, and an analyzer was placed behind the sample. The analyzer was rotated, and the transmitted power was measured using a power meter (PD300-3W, Ophir Optronics Solutions Ltd., Israel).

2.3. *TEM observation of bonding interface*

The microstructure of the bonded interfaces was observed using high-resolution transmission electron microscopy (TEM, JEM-2800, JEOL Ltd., Japan). Elemental mapping was performed by energy-dispersive X-ray spectroscopy (EDS) to identify constituent elements. To further understand the bonding mechanism, additional observations were conducted on sapphire/Nd:YAG single-crystal composite bonded under the same conditions as the ceramic composites. The specimens used for these observations were prepared from optically polished sapphire and Nd:YAG materials, obtained from their respective manufacturers and used as received.

Optical Materials EXPRESS

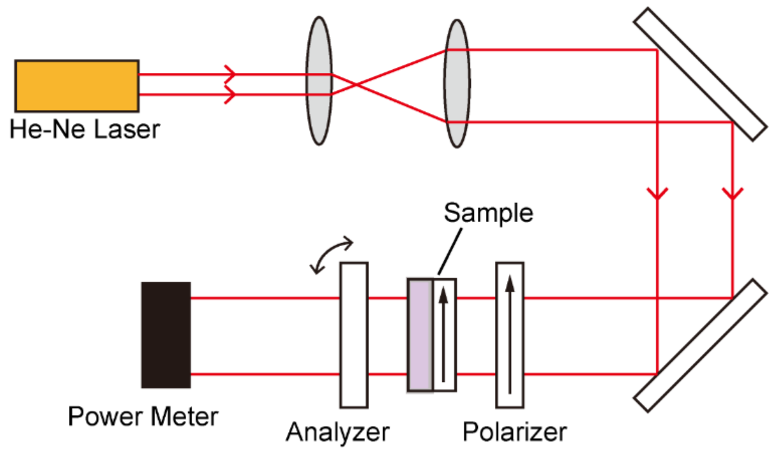

Fig. 2. Experimental setup for degree of polarization.

3. Results and discussion

3.1. Optical characteristics

Figure 3 shows photographs of Composite-1, Composite-3, and Composite-6. For samples with an initial surface flatness up to λ/5, all composites exhibited high-quality bonding; no interface fringes or cloudiness were observed. By contrast, the sides of Composite-6 (and Composite-7; λ-flatness samples) appeared to be poorly bonded, as indicated by the red arrow, which is likely due to the lower initial surface flatness of the Nd:YAG ceramics. However, within an aperture size of approximately 8 mm in Composite-6, bonding quality was sufficient, and the optical properties were comparable to those of the other composites.

Fig. 3. photographs of each bonded composite.

Figure 4 shows the transmission spectra for all composites. For improved readability, Fig. 4(a) and 4(b) present enlarged views around the excitation wavelength (808 nm) and lasing wavelength (1064 nm), respectively. At the excitation wavelength, no significant differences were observed among the composites. At the lasing wavelength, all composites except Composite-5 exhibited nearly identical transmittance values, ranging from 84.4% to 84.6%. These values were almost equal to the theoretical transmittance of the sapphire/YAG composite (84.7%), regardless of the initial surface flatness.

Table 2 summarizes the transmittance at 1064 nm and the transmitted wavefront (PV value) for all composites. The PV values ranged from 0.128λ to 0.264λ, and, similar to transmittance,

Optical Materials EXPRESS

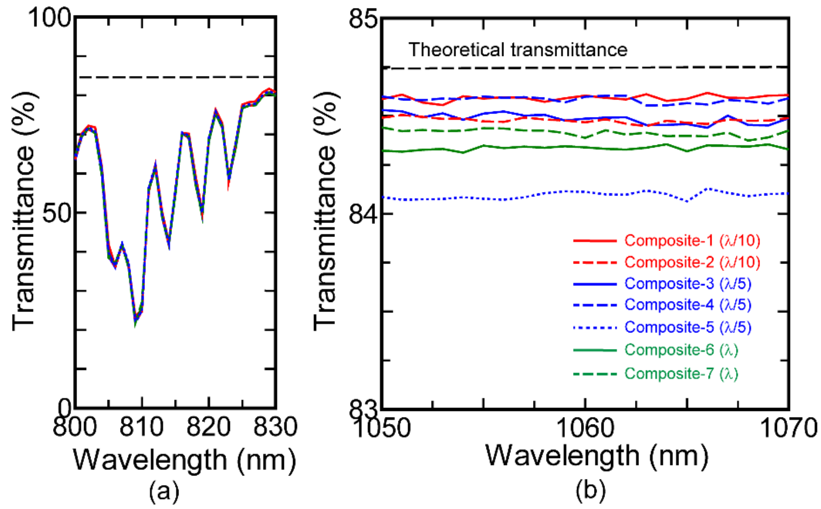

Fig. 4. Transmission spectra of all composites around the (a) excitation wavelength (808 nm) and (b) lasing wavelength (1064 nm).

showed no correlation with initial surface flatness. Typically, a transmitted wavefront of approximately λ/5 (i.e., 0.2λ) was obtained, indicating that the quality is sufficient for use as a laser material.

Table 2. Transmittance at 1064 nm and transmitted wavefront (PV value) for each composite. λ = **632.8 nm.**

Sample	Transmittance at 1064 nm (%)	Transmitted wavefront (λ)
Composite-1 (λ/10)	84.6	0.128
Composite-2 (λ/10)	84.5	0.259
Composite-3 (λ/5)	84.5	0.171
Composite-4 (λ/5)	84.6	0.264
Composite-5 (λ/5)	84.1	0.178
Composite-6 (λ)	84.4	0.213
Composite-7 (λ)	84.4	0.220

Figure 5 shows the transmitted power and extinction ratio of the composites. The degrees of polarization for the He-Ne laser (without composite), Composite-1, Composite-3, and Composite-6 were 41.9 dB, 34.3 dB, 32.0 dB, and 35.0 dB, respectively. These results indicate that depolarization in the composites was negligible, implying minimal residual stress inside the composites. Therefore, appropriate bonding can be achieved even when the initial surface flatness of the YAG ceramics is around λ, which is highly advantageous for large-aperture applications.

3.2. Laser characteristics

To compare the laser performance of composites with different initial surface flatness, we conducted laser oscillation tests. Figure 6 shows the experimental setup for the lasing test. The cavity length was approximately 25 mm, comprising a flat dichroic mirror and a concave laser output coupler ($R = 50$ mm). The reflectivity of the output coupler was 95%. A continuous-wave (CW) 60 W fiber-coupled laser diode (LD) with a core diameter of 105 µm was used as the pump source. The LD output was focused onto the Nd:YAG ceramics with a spot diameter of approximately 105 µm, and the laser output power was measured using a power meter (30A,

Optical Materials EXPRESS

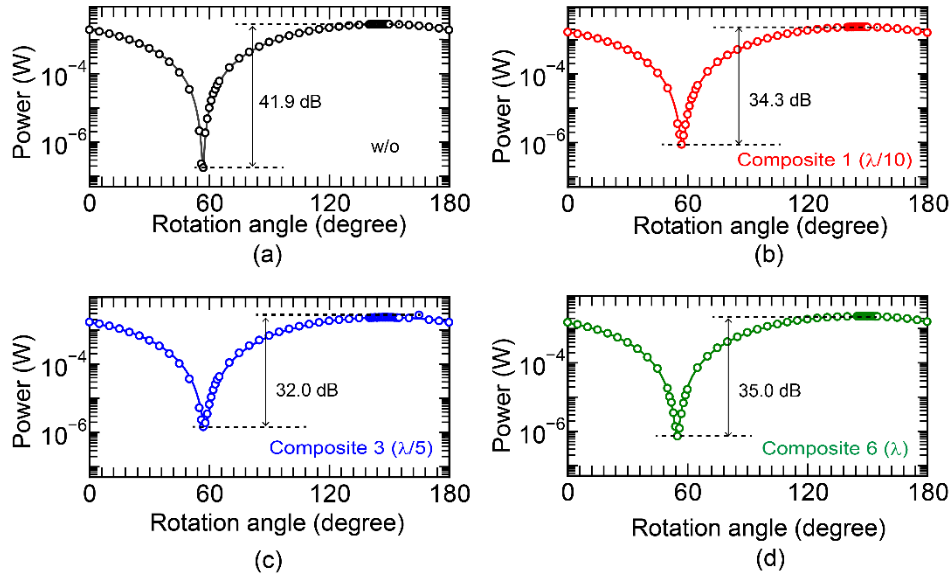

Fig. 5. Degree of polarization of the probe beam (w/o composite) and for each bonded composite.

Ophir Optronics Solutions Ltd., Israel). For this measurement, composite samples 1, 3, and 6 (listed in Table 1) were tested. For comparison, a single-piece Nd:YAG ceramic was also measured. The cavity configuration, including the LD focusing point, was kept fixed and only the sample was replaced to ensure a fair comparison. Consequently, the sample position was approximately fixed within the laser cavity.

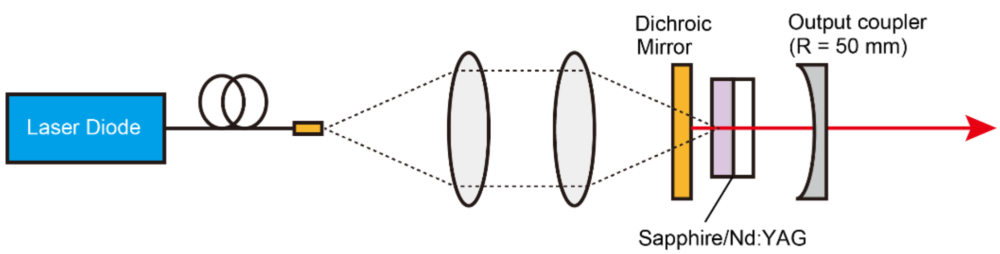

Fig. 6. Experimental setup for laser oscillation.

Figure 7 shows the laser output characteristics of the composite materials. As the excitation power increases up to 10 W, the output power of all samples initially increases. Beyond this point, the output power of the unbonded Nd:YAG ceramics (without sapphire) decreases more rapidly than that of the bonded composites, most likely owing to thermal effects. In the bonded samples, the decrease occurs at higher excitation powers, resulting in an output improvement of approximately 13% compared to the unbonded ceramics at high power. This enhancement can be attributed to the conductive cooling effect provided by sapphire, as reported in our previous study [3].

Furthermore, no significant differences were observed in the laser outputs among the composite materials. The slope efficiency was evaluated using data points for excitation powers up to 12 W, as shown in Fig. 7. Both the lasing threshold and slope efficiency were nearly identical for all samples, indicating that total cavity losses, including those from the laser medium, were similar.

Optical Materials EXPRESS

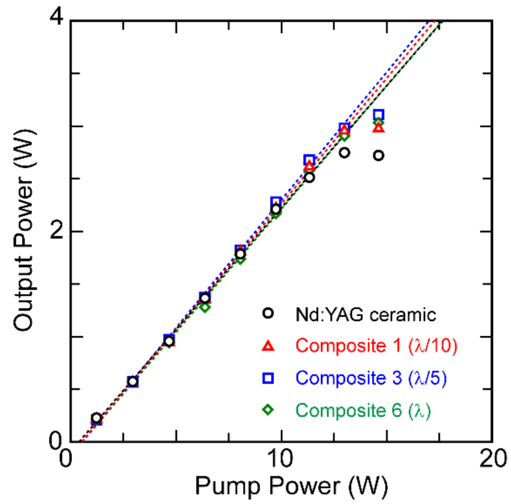

Fig. 7. Laser output power as a function of pump power for single Nd:YAG ceramics and bonded composites.

Therefore, the optical loss at the bonded interfaces can be considered negligibly small, which is consistent with the transmittance results shown in Fig. 4.

In the experiments, the decrease in laser output under high pump power, which is attributed to thermal effects, occurred at nearly the same pump power for all bonded composites, regardless of the initial surface flatness. This suggests that thermal management is not significantly influenced by surface flatness within the range investigated. Although additional characterization (for example, far-field beam profiles and detailed wavefront measurements) would be required for further clarification, which will be addressed in the future studies, the results obtained in this study indicate that pulsed electric current bonding of sapphire/Nd:YAG ceramics is insensitive to initial flatness with respect to laser output characteristics.

3.3. TEM observations

Figure 8 shows TEM images of the sapphire/Nd:YAG ceramic composites interfaces. For comparison, similar observations were conducted on the sapphire/Nd:YAG single-crystal composite. As shown in Fig. 8(a), in the case of Nd:YAG ceramics, an interlayer approximately 20 nm thick was clearly observed at the interface. This interlayer was not detected in our previous study using FE-SEM due to its limited resolution [3]. TEM analysis revealed that the interlayer was crystalline. By contrast, as shown in Fig. 8(b), no such interlayer was observed at the single-crystal composite interface, indicating that interlayer formation is characteristic of bonding with ceramics.

Figure 9 presents the elemental mapping results of the sapphire/Nd:YAG ceramic interface obtained by EDS. The interlayer consists of Y, Si, O, and Nd, with almost no Al detected. The Si is likely derived from sintering additives in the YAG ceramics. Previous studies have shown that Si can diffuse during heat treatment via grain boundary diffusion [20–22], leading to its accumulation at the sapphire interface, where it may form a Y–Si complex oxide, such as yttrium silicate.

Although the interlayer at the sapphire/Nd:YAG ceramic interface could potentially act as a light-scattering source, its small thickness (approximately 20 nm) did not cause significant optical loss. Furthermore, high-quality bonding was also achieved at the sapphire/Nd:YAG single-crystal interfaces, suggesting that successful direct bonding of dissimilar materials does not depend on

Optical Materials EXPRESS

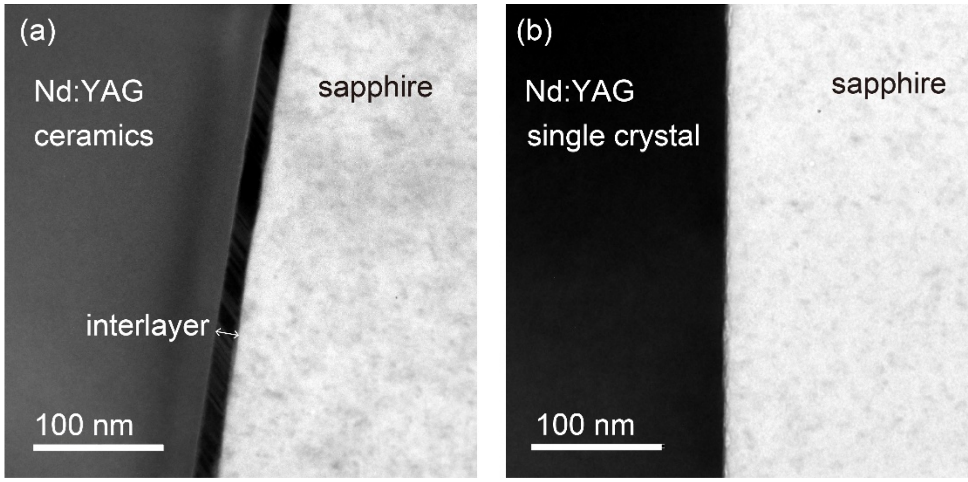

Fig. 8. TEM images of the bonded interfaces for (a) sapphire/Nd:YAG polycrystalline ceramics and (b) sapphire/Nd:YAG single crystal.

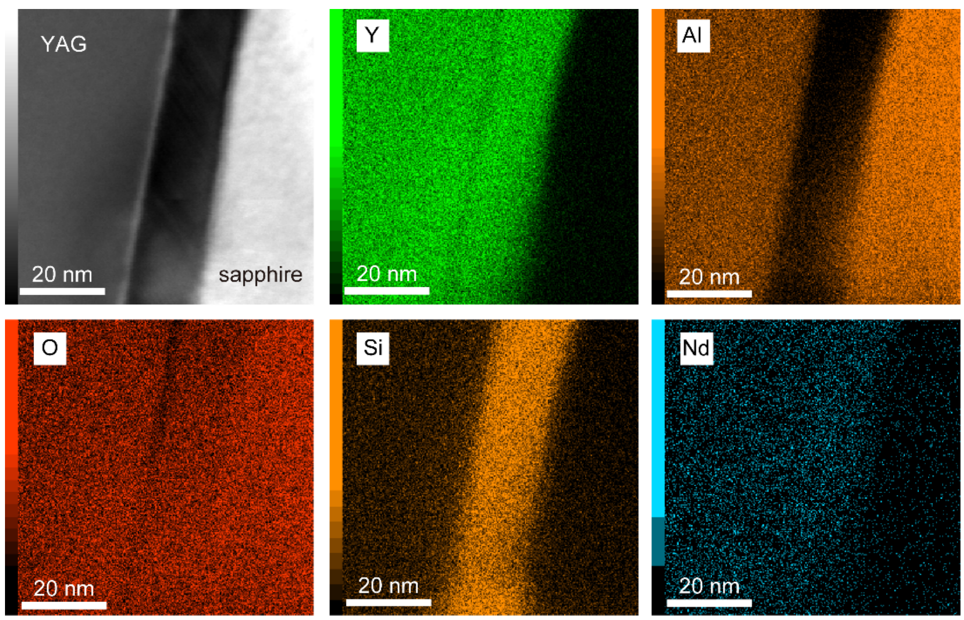

Fig. 9. EDS elemental mapping of sapphire/Nd:YAG ceramics composite interface.

interlayer formation. This finding provides valuable insights for bonding not only different types of substrates but also similar ceramic materials using thermal diffusion bonding by PECB.

4. Conclusion

In this study, we investigated flatness-insensitive pulsed electric current bonding (PECB) of sapphire and Nd:YAG ceramics for high-average-power laser applications. Nd:YAG ceramics with varying initial surface flatness levels (λ/10, λ/5, and λ) were bonded to sapphire, and no significant differences were observed in in-line transmittance, transmitted wavefront, degree of

Optical Materials EXPRESS

polarization, or laser performance over most of the bonded area. These results demonstrate that high-quality bonding can be achieved even when the initial surface flatness is approximately λ, highlighting the feasibility of using PECB for large-aperture optical elements—a significant advantage over conventional bonding methods.

Notably, the present experiments were conducted using relatively small-diameter samples (ϕ10 mm). Further studies with large-diameter samples are necessary to confirm these findings. Additionally, TEM observations revealed the accumulation of silicon from the sintering additives and the formation of an interlayer approximately 20 nm thick, which was not observed in samples bonded to Nd:YAG single crystal.

Future work will focus on bonding with *c*-cut sapphire (which exhibits no polarization dependence), developing sandwich structures, and scaling up to large-aperture samples. These investigations are expected to enhance understanding and promote the practical application of flatness-insensitive PECB in high-average-power laser development.

Funding. National Institute for Fusion Science (NIFS25KIII021, NIFS23KIIH019).

Disclosures. The authors declare no conflicts of interest.

Data availability. The data underlying the results presented in this paper are not publicly available at this time but may be obtained from the authors upon reasonable request.

References

1. H. Ichikawa, K. Yamaguchi, T. Katsumata, *et al.*, "High-power and highly efficient composite laser with an anti-reflection coated layer between a laser crystal and a diamond heat spreader fabricated by room-temperature bonding," Opt. Express **25**(19), 22797–22804 (2017).
2. L. Zheng, A. Kausas, and T. Taira, "Drastic thermal effects reduction through distributed face cooling in a high power giant-pulse tiny laser," Opt. Mater. Express **7**(9), 3214–3221 (2017).
3. H. Furuse, Y. Koike, and R. Yasuhara, "Sapphire/Nd:YAG composite by pulsed electric current bonding for high-average-power lasers," Opt. Lett. **43**(13), 3065–3068 (2018).
4. Y. Chen, Y. Lin, J. Huang, *et al.*, "Efficient continuous-wave and passively Q-switched pulse laser operations in a diffusion-bonded sapphire/Er:Yb:$YAl_3(BO_3)_4$/sapphire composite crystal around 1.55 µm," Opt. Express **26**(1), 419–427 (2018).
5. Z. Feng, C. Ma, S. Hu, *et al.*, "Transparent YAG ceramic/sapphire composite fabricated by pressureless direct thermal diffusion bonding," J. Eur. Ceram. Soc. **41**(15), 7845–7851 (2021).
6. K. Fujioka, X. Guo, M. Maruyama, *et al.*, "Room-temperature bonding with post-heat treatment for composite Yb:YAG ceramic lasers," Opt. Mater. **91**, 344–348 (2019).
7. L. Zheng, A. Kausas, and T. Taira, ">30 MW peak power from distributed face cooling tiny integrated laser," Opt. Express **27**(21), 30217–30224 (2019).
8. I. Kuznetsov, A. Pestov, I. Mukhin, *et al.*, "Composite Yb:YAG/sapphire thin-disk active elements for high-energy high-average power lasers," Opt. Lett. **45**(2), 387–390 (2020).
9. A. Kausas and T. Taira, "Laser-induced damage study of bonded material for a high-brightness laser system," Opt. Lett. **47**(12), 3067–3070 (2022).
10. Y. Sato, A. Kausas, and T. Taira, "Enhanced thermal conductivity of distributed face-cooled composite laser medium included thermal resistance at the bonding interface," Opt. Express **33**(11), 24039–24049 (2025).
11. V. Yahia, A. Kausas, A. Tsuji, *et al.*, "Joule-class sub-nanosecond pulses produced by end-pumped direct bonded YAG/sapphire modular amplifier," Opt. Express **32**(8), 14377–14393 (2024).
12. P. Mason, M. Divoký, K. Ertel, *et al.*, "Kilowatt average power 100 J-level diode pumped solid state laser," Optica **4**(4), 438–439 (2017).
13. M. Divoký, J. Pilař, M. Hanuš, *et al.*, "150 J DPSSL operating at 1.5 kW level," Opt. Lett. **46**(22), 5771–5773 (2021).
14. T. Sekine, T. Kurita, Y. Hatano, *et al.*, "253 J at 0.2 Hz, LD pumped cryogenic helium gas cooled Yb:YAG ceramics laser," Opt. Express **30**(25), 44385–44394 (2022).
15. Y. Yu, W. Zhu, Y. Ma, *et al.*, "Novel design of sapphire/spinel transparent ceramic joints with double glass interlayers by coating and bonding," Ceram. Int. **50**(1), 1591–1600 (2024).
16. M. Sakajio, N. Pears, M. Dov, *et al.*, "Glass bonding of YAG/Nd:YAG and Sapphire/Nd:YAG windows," Opt. Mater. **151**, 115363 (2024).
17. J. Lin, P. Lin, R. Ao, *et al.*, "Microstructure evolution and mechanical properties of YAG/YAG joint using bismuth-borate glass," J. Eur. Ceram. Soc. **41**(4), 2847–2854 (2021).
18. W. Zhu, Y. Chen, H. Zou, *et al.*, "Microstructure, mechanical and optical properties of $MgAl_2O_4$/$MgAl_2O_4$ joints bonded using CaO-Al_2O_3-SiO_2 glass filler," J. Eur. Ceram. Soc. **42**(6), 2994–3003 (2022).
19. X. Liu, D. Han, X. Mao, *et al.*, "Joining transparent spinel ceramics using refractive index–matched glass," J. Eur. Ceram. Soc. **42**(8), 3579–3585 (2022).

Optical Materials EXPRESS

20. R. Boulesteix, A. Maître, J. F. Baumard, *et al.*, "The effect of silica doping on neodymium diffusion in yttrium aluminum garnet ceramics: implications for sintering mechanisms," J. Eur. Ceram. Soc. **29**(12), 2517–2526 (2009).
21. K. Fujioka, A. Sugiyama, Y. Fujimoto, *et al.*, "Ion diffusion at the bonding interface of undoped YAG/Yb:YAG composite ceramics," Opt. Mater. **46**, 542–547 (2015).
22. K. Fujioka, T. Mochida, Y. Fujimoto, *et al.*, "Heat treatment of transparent Yb:YAG and YAG ceramics and its influence on laser performance," Opt. Mater. **79**, 353–357 (2018).